Power and Efficiency of Salient Pole and Flux Barrier Type Synchronous Reluctance Machines in Low Power Drives

Matthias Hofer, Mario Nikowitz, Manfred Schrödl
Technische Universität Wien, Institute of Energy Systems and Electrical Drives
Gußhausstraße 25-27
A-1040 Vienna, Austria
Phone: +43 1 58801-370230
Email: matthias.hofer@tuwien.ac.at
URL: http://www.tuwien.ac.at

Keywords

≪AC-Machine≫≪Synchronous Motor≫, ≪Variable Speed Drive≫, ≪Adjustable Speed Drive≫, ≪Efficiency≫.

Abstract

In this paper synchronous reluctance machine topologies are investigated regarding power and efficiency for a low power industrial drive. Starting from an existing standard induction motor two rotor types, flux barrier and salient pole, were designed for a wide speed range of the electric drive. By adaptation of the stator winding the drive requirements are met for both topologies. In this work the focus is set to the behavior in the flux weakening region for utilizing a high power capability and high efficiency in an application. Both rotor types are analyzed by finite element methods and show different characteristics. The salient pole machine is able to provide a power at maximum speed more than two times higher than the flux barrier type and shows a much broader constant power speed range. Further, because of nearly constant machine saliency, the part load efficiency of the salient pole rotor is higher, although the flux barrier machine has a higher efficiency at maximum torque. Experimental results are presented and confirm the higher torque per ampere characteristic of the salient pole machine because of its lower quadrature axis inductance. The torque vs. speed limit during flux weakening shows the higher performance of the salient pole rotor. Thus, in this application at driving cycles with major operation time at high speeds the salient pole rotor is preferred.

Introduction

Synchronous reluctance machines (SynRM) are characterized by a simple and robust rotor structure. Due to the lack of permanent magnets or rotor windings this machine is attractive for low cost applications. SynRMs have lower rotor losses and lower product costs compared to Induction Machines (IM) or Permanent Magnet Synchronous Machines (PMSM). As shown in [1] and [2] SynRMs provide higher torque density at same efficiency or a higher efficiency at same machine volume compared to IMs. Therefore, SynRMs are proposed by some electric machine manufacturers to meet efficiency requirements according to the IEC 60034-30 standard. For existing variable speed drives (VSD) with field oriented controlled (FOC) IMs, SynRMs are a potential replacement with higher efficiency. In [3] a SynRM is investigated even for IE5 efficiency class. In [4] different machine types are evaluated for the IE efficiency classes. Herein, for sinusoidal field SynRM the IE4 level is applicable, but for the Ultra-Premium Efficiency Class (IE5) difficulties for some power ratings and standardized frame sizes are expected. Thus, the replacement of IMs by SynRMs is ongoing research work to reach highest efficiency in electrical machines and drives in future.

Generally, efficiency is rather low at low power machines. Depending on the machine power and operational speeds the IE4 efficiency requirement for machines with low rated power, e.g. 120W or 180W are in the range of only 65% to 75% for the nominal load condition. In contrast, variable speed drives are operated in different speed and torque ranges. Therefore, any efficiency evaluation for characterization has to consider various load conditions. For variable speed drives several selected torque and speed values are combined to evaluate the efficiency according to the IEC 60034-30-2 standard. This standardized method shows the importance of an overall loss consideration during the operation. Definitely, selected load points can not represent the energy consumption during real driving cycles. But finally, the part load efficiency of machines and drives becomes of higher interest already today and in future.

The SynRM's working principle is based on different magnetic resistances in the direct and quadrature axis of the SynRM rotor. In contrast to IMs or PMSMs the rotor consists only of soft magnetic material (usually laminated steel) and a special geometry to realize magnetic saliency. For SynRMs two different rotor architectures are known. The flux barrier (FB) topology uses internal holes at a cylindrical rotor shape. In contrast, the salient pole (SP) machine has a non-cylindrical shape and provides the reluctance by different airgap length along the rotor circumference. Consequently, these different rotor types lead to different machine characteristics. In this work, both rotor types are compared as an alternative for the used IM drive. A four pole standard IM (size 63) is the basis of this investigation. In this application the drive is operated also in the flux weakening range. The objective of this work is to improve the machine power and efficiency by utilizing a SynRM rotor. Therefore, the stator geometry and overall machine dimensions remain unchanged from the IM. A stator winding adjustment is possible, but manufacturing tools and production processes have to be reused. For such a SynRM approach a cost reduction with a higher machine performance is expected.

An additional potential for reducing product costs at high efficiency is the application of sensorless control to the SynRM drive. The sensorless rotor position can be evaluated by high frequency harmonic injection (e.g. in [5]) or with transient voltage pulse injections as in [6]. In [7] and [8] this approach was applied successfully. A sufficient sensorless control of SynRMs requires a high saliency ratio even at zero current [9]. Therefore, salient pole machines are recommended for sensorless SynRM drives.

The application considered in this work has two key requirements:

- Torque $M = 0.6$Nm at phase current $I = 1.5A_{rms}$.
- Power $P = 50$W up to $6000min^{-1}$ at line voltage $U = 162V_{rms}$.

The machine efficiency, especially during the operation in the application's driving cycle, shall be has high as possible. For convenience, the machine efficiency is discussed based on the ohmic losses in the design phase. First, the SynRM machine model is presented. Furthermore, simulation results of the FB and SP machine performance are investigated regarding these requirements. Finally, the machine characteristic is tested with real prototypes.

1 Synchronous Reluctance Machine Model

At SynRMs only the stator winding provides the ampereturns for flux generation. The rated stator flux linkage $\underline{\Psi}_S = \Psi_{S,d} + j\Psi_{S,q}$ depends only on the rated stator current $\underline{I}_S = I_{S,d} + jI_{S,q}$ with neglecting cross coupling inductances as

$$\Psi_{S,d} = L_d(I_{S,d}) \cdot I_{S,d} \tag{1}$$

$$\Psi_{S,q} = L_q(I_{S,q}) \cdot I_{S,q}. \tag{2}$$

Depending on the machine type and design, the inductances are generally not constant and are described as a function of the currents $I_{S,d}$ and $I_{S,q}$. The machine torque M depends on the direct and quadrature inductances L_d and L_q and on the stator current components. For a high torque generation the inductance

Assigned jointly to the European Power Electronics and Drives Association & the Institute of Electrical and Electronics Engineers (IEEE)

difference $L_d - L_q$ should be high and both current components $I_{S,d}$ and $I_{S,q}$ have to be applied necessarily.

$$M = \frac{3}{2} p \ (L_d - L_q) \ I_{S,d} \ I_{S,q} \tag{3}$$

Further, using the current angle $\Theta = \arg\{\underline{I}_S\}$ the torque equation yields

$$M = \frac{3}{2} p \ (L_d - L_q) \ |\underline{I}_S| \cos\Theta \ |\underline{I}_S| \sin\Theta \tag{4}$$

$$= \frac{3}{4} p \ (L_d - L_q) \ |\underline{I}_S|^2 \sin(2\Theta) \tag{5}$$

In the voltage equations

$$U_{S,d} = I_{S,d} \ R_S + L_d(I_{S,d}) \frac{dI_{S,d}}{dt} - \Omega_e \ L_q(I_{S,q}) \ I_{S,q} \tag{6}$$

$$U_{S,q} = I_{S,q} \ R_S + L_q(I_{S,q}) \frac{dI_{S,q}}{dt} + \Omega_e \ L_d(I_{S,d}) \ I_{S,d} \tag{7}$$

a cross coupling of both current components can be identified. This aspect is important for a sufficient operation in transient load cases and operation in the flux weakening range because cross coupling increases with higher electric frequency Ω_e.

2 Flux Barrier Machine

Flux barrier (FB) rotors have a cylindrical rotor shape and provide the saliency by internal holes or slots. For electromagnetic reasons the circumferential ribs should be as small as possible but due to centrifugal forces and manufacturing limitations a compromise has to be chosen. In the works [9],[10],[11] the flux barrier arrangement (number and shape) is investigated with respect to a high strength and a high saliency. For this application a four pole FB rotor with three flux barriers was designed for the existing stator and the prototype was built, see Fig. 1.

The design and performance analysis is done with a 2D finite element model. Iron losses, friction losses and additional losses are not considered. To meet the torque and power requirements, the stator winding is adjusted with N=63 and a Y-connection is used. The machine performance is presented in Fig. 3 and Fig. 4.

Fig. 1: Prototype rotor of the FB machine with three barriers.

Fig. 2: Rotor lamination stack of the continuously skewed salient pole rotor.

At low speeds the machine is operated in MTPA mode (Maximum Torque per Ampere) up to n_{I-II}= $2450 min^{-1}$ (region I) where the voltage limit $|\underline{U}_S|$ is reached. As expected, a constant maximum torque and increasing power according to Fig. 3 can be seen. For higher speeds the Maximum Torque per

Volt (MTPV) strategy is applied. A small constant power speed range (CPSR) with power $> 160W$ in region II is given. The voltage and current magnitude remain constant to achieve maximum torque and the current angle Θ increases from $47°$ up to nearly $70°$. At speeds higher than n_{II-III}=3700min^{-1} the current magnitude as well as the power decreases (Fig. 4) and Θ increases further up to $76°$. The desired power of $50W$ at $6000min^{-1}$ is just reached. Further, in region III the phase angle (between current and voltage) increases and leads to a very low power factor (e.g. $cos(70°) \approx 0.34$) in flux weakening range of the FB type SynRM.

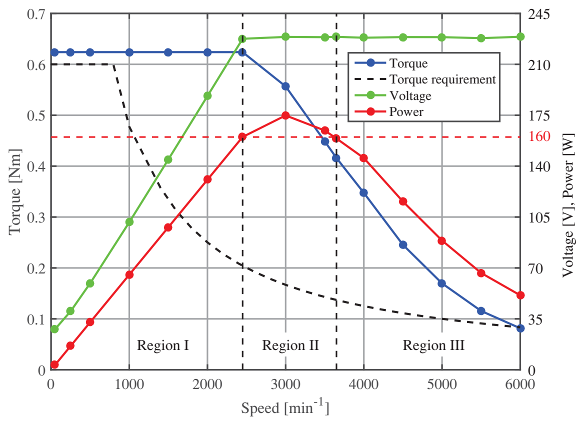

Fig. 3: Simulated torque, power and voltage of the FB rotor depending on speed, given stator with N=63 turns in Y-connection.

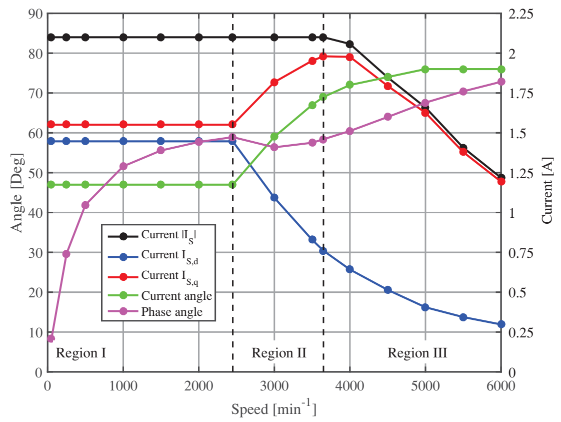

Fig. 4: Simulated current, current angle and phase angle of the FB rotor depending on speed, given stator with N=63 turns in Y-connection.

3 Salient Pole Machine

In a previous work the design of a salient pole machine was investigated for a Δ-connected stator winding [12]. To keep the single layer stator winding this configuration is adjusted to a Y-connection winding. By unequal pole angles and a continuous rotor skewing by one stator slot pitch a sufficient low harmonic behavior is achieved. Details about the machine design are given in [13]. The four pole SP design is shown in Fig. 2.

In the base speed range the machine provides the same output power as the FB type, see Fig. 5. To achieve this behavior, the number of stator turns was adjusted with N=70. The MTPV range starts at n_{I-II}=2850min^{-1} and also leads to a higher output power. The CPSR with power $> 185W$ lasts to n_{II-III}= 5000min^{-1}. With this wider CPSR only for the last 1000min^{-1} the current needs to be reduced. Even at maximum speed the machine generates $\approx 150W$, which is three times higher than the requirement. Because of the wide CPSR the phase angle (Fig. 6) is not bigger than $55°$ and lead to a higher power factor ((e.g. $cos(55°) \approx 0.57$) compared to the FB machine.

4 Efficiency and Power Comparison

After presentation of the machine power/speed range, the machine efficiency is discussed in this section. A different behavior of both machines is expected because according to equation (5) the inductance characteristic has a major impact on the machine torque. The current vs. torque characteristic for both designs is compared in Fig. 7. Because of the winding adjustment the machines have the same torque at maximum current 2.1A$_{peak}$. The salient pole machine provides a higher torque per ampere at low currents because the inductances L_d and L_q of this machine type are nearly constant and only defined by its geometry. In contrast, at FB rotors the small bridges have to saturate first until a high saliency is given. Thus, the inductances, especially L_q, significantly depend on saturation. Therefore, the machine torque first remains rather low and only after at a certain current of approx. 0.5A a torque increase can be seen, which is higher than at the SP rotor. By this characteristic a higher efficiency of the SP in part load operation is given.

 ISBN: 978 - 9 - 0758 - 1528 - 3 - IEEE catalog number: CFP18850-ART
Assigned jointly to the European Power Electronics and Drives Association & the Institute of Electrical and Electronics Engineers (IEEE)

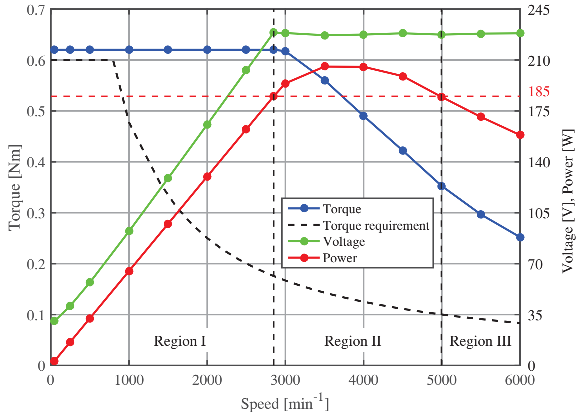

Fig. 5: Simulated torque, power and voltage of the SP machine depending on speed, given stator with N=70 turns in Y-connection.

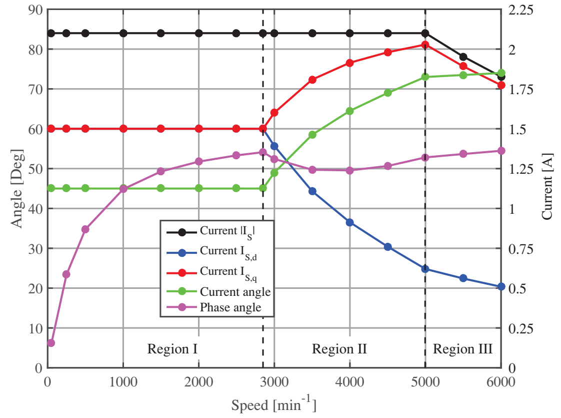

Fig. 6: Simulated current, current angle and phase angle of the SP machine depending on speed, given stator with N=70 turns in Y-connection.

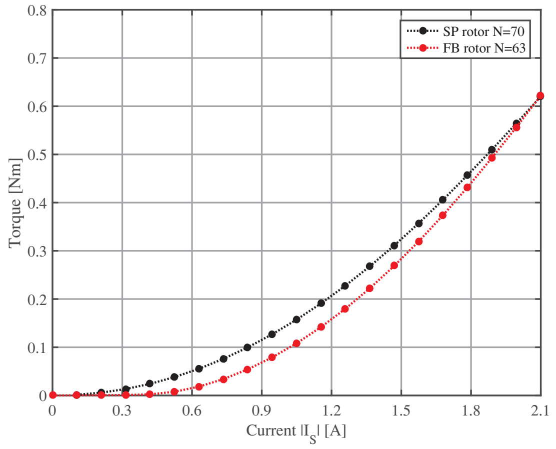

Fig. 7: Current vs. torque characteristic of FB and SP rotor.

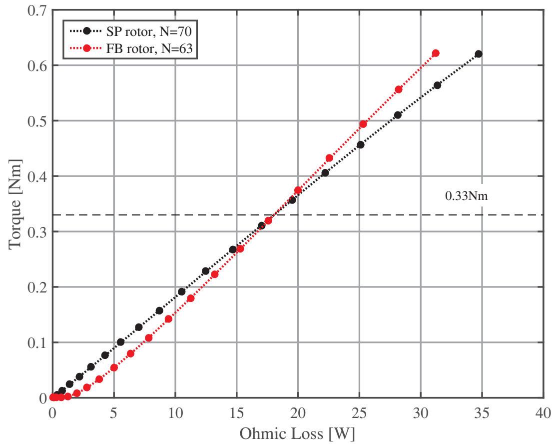

Fig. 8: FB and SP ohmic loss vs. torque.

The different number of stator winding turns leads to phase resistances $R_{S,SP}$=7.87Ω and $R_{S,FB}$=7.09Ω. In Fig. 8 the ohmic stator losses are shown in relation to the machine torque, each for MTPA operation. At the SP machine a linear behavior is identified, because ohmic loss as well as the torque are proportional to $|\underline{I}_S|^2$, see equation (5), where inductances L_d and L_q are nearly constant (see also Fig. 11). At the FB machine, especially the variable inductance L_q leads to the shown characteristic with higher losses at low torques. In the range of $M < 0.33$Nm the SP rotor performs better with regard to the ohmic losses.

A simplified efficiency consideration for high and low torques is shown in Fig. 9 and Fig. 10. The efficiency is evaluated only based on ohmic losses. Iron losses, friction losses and additional losses are not considered, because first the relation of both machines to each other is of interest and the overall efficiency will be investigated during driving cycles. These loss portions are assumed to be similar, due to the common stator geometry, same operational frequencies and same mechanical setup. The SP machine can be operated at 0.1Nm up to full speed in MTPA mode, see Fig. 9. The FB machine has a lower efficiency and MTPA mode is limited at approx. $4500min^{-1}$. At maximum torque (Fig. 10) the efficiency is higher at the FB rotor. Because of a higher output power the efficiency advantage of the FB machine is rather small compared to the low torque range. Further, here the SP type can also operate at higher speeds in MTPA mode up to $2850min^{-1}$. At the end of the base speed range n_{I-II} for each machine the efficiency is quite the same. Further, with this simplified efficiency the SP type efficiency is the same for all torques because of the quadratic relation of current to losses and current to torque or power.

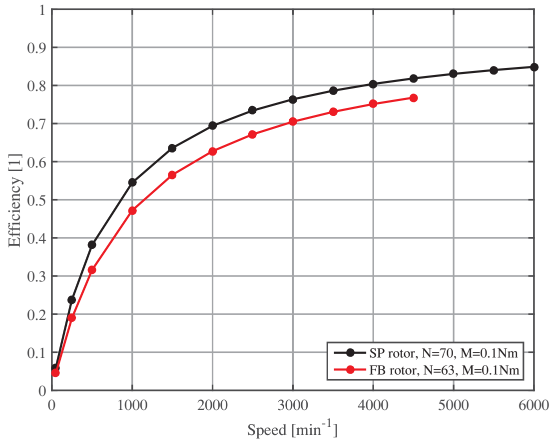

Fig. 9: FB and SP efficiency (without iron loss, friction loss and additional losses) at 0.1Nm torque (part load) in MTPA mode.

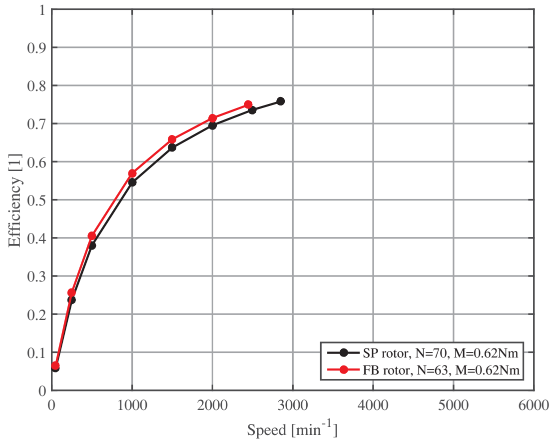

Fig. 10: FB and SP efficiency (without iron loss, friction loss and additional losses) at 0.62Nm torque (full load) in MTPA mode.

Finally, for this application the focus on low power operation up to 50W results in the preference to the SP machine. In a major operation region the SP machine benefits of the higher part load efficiency. Only during machine start at maximum torque efficiency is a little lower than at the FB type. Further, the flux weakening operation can be implemented in pure MTPA mode and simplifies the drive control, because the current angle Θ remains constant. An additional cost reduction potential is the application of sensorless control, which is much easier at the SP machine than at the FB type.

Experimental Results

The major difference between SP and FB SynRMs is the inductance characteristic, see Fig.11. The rated inductance $l_q(i_q)$ of the SP rotor is independent of the current level, because it is mainly characterized by the large airgap in q-axis direction. In contrast, at the FB rotor at low currents the inductance l_q is high because the rotor bridges are not saturated yet. At increasing current levels saturation in quadrature axis arises and the inductance decreases accordingly. This measured characteristic matches the theoretical analysis. In the direct axis both rotors have similar characteristic and the inductance $l_d(i_d)$ decreases at higher currents for both rotor types. Finally, the FB machine has a lower saliency in part load operation because of the higher quadrature inductance.

The machine saliency affects the torque to current behavior according to equation (5) as already investigated in Fig. 7. The experimental result is presented in Fig. 12 accordingly. The real machine prototypes deliver different torque at nominal current $|i_S| = 1$ although they are designed for same torque at nominal current. The maximum torque of the SP machine is $M_{SP} = 0.72$Nm and $M_{FB} = 0.6$Nm at the FB type. Thus, for comparison, the rated torque at nominal current is taken into account instead of the absolute torque value. As expected, the SP rotor benefits from the higher saliency ratio in part load operation, where the rated torque is higher than at the FB type. Only at overload conditions $|i_S| > 1$ the FB generates more torque per current. The optimal current angle at nominal current was identified as $\Theta_{SP} = 47°$ for the SP rotor and $\Theta_{FB} = 45°$ for the FB rotor.

The machine characteristics of the FB and SP rotor type were tested also in flux weakening operation at maximum line to line voltage ($U = 162V_{rms}$). Experimental results in MTPA as well as in MTPV operation are depicted in Fig. 13 for the FB rotor and in Fig. 14 for the SP type. A comparison with the simulation (Fig. 3 and Fig. 5) shows a good matching of the general characteristic. The FB rotor can reach the required torque at $6000min^{-1}$ only in MTPV mode, in MTPA mode the torque is quite below the requirement. The SP machine reaches the required load curve even in MTPA operation and provides even the doubled power in MTPA mode than required. This is advantageous for the drive efficiency as well as for machine control. Thus, during flux weakening the control angle stays constant at $\Theta_{SP} = 47°$ and only the stator current has to be reduced at increasing speed. Further, a small torque margin from the

MTPA to requirement is still given which provides a stator voltage reserve either for dynamic operation or possible voltage deviations in the application. Comparison of the machine power shows a significant power increase of the SP rotor especially in flux weakening and at the maximum power point. At both machines the corner speed is at $2880min^{-1}$. The FB machine has a small CPSR from from $2880min^{-1}$ to $3500min^{-1}$ with a power >181W. The SP prototype has a wider CPSR from $2880min^{-1}$ to $4750min^{-1}$ with a higher power of >218W. The SP machine provides maximum 236W at $3500min^{-1}$. These results show the high potential of the SP rotor type SynRM as a future replacement of the currently used IM within the same package and even with same stator stack geometry.

The investigation of the drive efficiency is important to be done during real driving cycles of the target application. As the maximum load profile (torque requirement according to Fig.13 and Fig. 14) is mainly lower than the 0.33Nm and the machine is operated mainly at constant power operation, a clear advantage is expected for the SP rotor. First tests within the application are currently running and results of the driving cycle efficiency will be presented in future work.

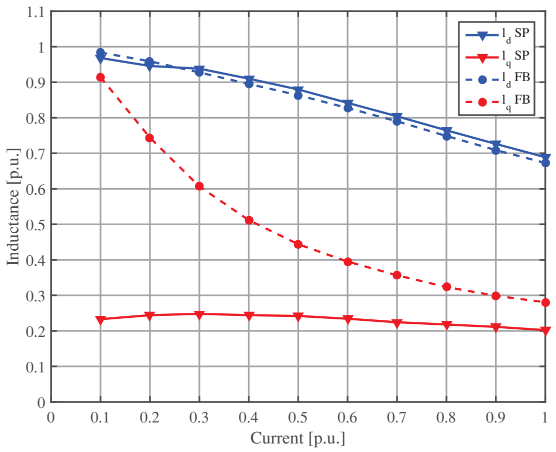

Fig. 11: Measured inductances of the FB and SP prototype.

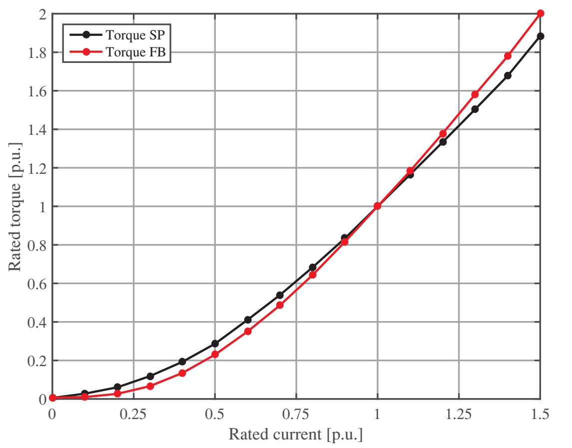

Fig. 12: Measured rated torques of the FB and SP prototype.

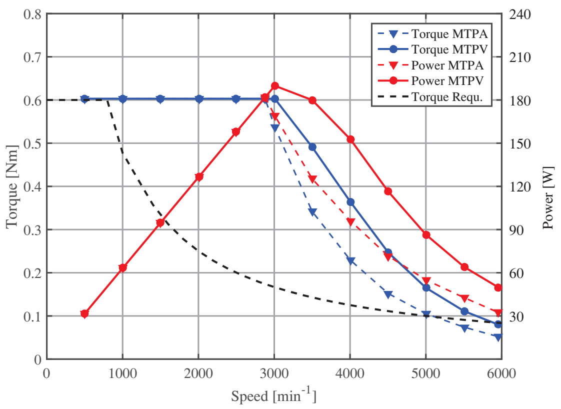

Fig. 13: Measured torque and power of the FB prototype in MTPA and MTPV mode.

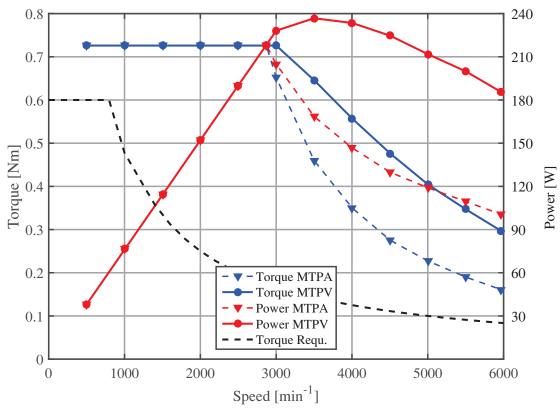

Fig. 14: Measured torque and power of the SP prototype in MTPA and MTPV mode.

Conclusion

In this work two different approaches of synchronous reluctance rotor topologies are discussed. The machine performance for a low power industrial drive with wide constant power demand is analyzed by finite element simulation and first experimental results with prototypes are presented. With a common stator geometry and an adjusted single layer stator winding the drive requirements can be fulfilled easily with the salient pole machine and only just reached with the flux barrier rotor. Both machines are designed to reach the same torque at maximum current. Therefore, the stator winding has a different number of turns.

The salient pole machine can be fully operated in MTPA mode including the flux weakening range for these drive requirements. Thus, a higher efficiency also in the high speed region can be realized. Further, the salient pole type shows a higher part load efficiency for torques approximately less than half of maximum torque. At high torques the salient pole machine shows higher copper losses because of different stator resistance. Nevertheless, the salient pole machine has clear advantages for this application with high rotational speeds. Experimental results confirmed the enlarged power capability of the salient pole machine and higher torque per current ratio especially at low torques. In addition, the salient pole machine offers the potential application of sensorless control without any pre-saturating current to ensure saliency. Experimental evaluation on the efficiency is ongoing work, but based on the previous results also a higher efficiency of the salient pole rotor during real driving cycles is expected.

References

[1] Almeida A.T. de, Ferreira F.J.T.E., Baoming G.: Beyond Induction MotorsTechnology Trends to Move Up Efficiency, ,IEEE Transactions on Industry Applications,vol. 50, no. 3, May/June 2014
[2] Boglietti A., Pastorelli M.: Induction and synchronous reluctance motors comparison, The 34th Annual Conference of IEEE Industrial Electronics, pp. 2041-2044, IECON 2008
[3] Dmitrievskii V., Prakht P., Kazakbaev V., Oshurbekov S., Sokolov I.: Developing ultra premium efficiency (IE5 class) magnet-free synchronous reluctance motor, The 6th International Electric Drives Production Conference (EDPC), 2016
[4] Almeida A.T. de, Ferreira F.J.T.E., Duarte A.Q.: Technical and Economical Considerations on Super High-Efficiency Three-Phase Motors, IEEE Transactions on Industry Applications, vol. 50 no. 2, 2014
[5] Morandin M., Da Ru D., Bolognani S., Bianchi N.: An Integrated Starter-Alternator Based on a Sensorless Synchronous Reluctance Machine Drive, IEEE Vehicle Power and Propulsion Conference (VPPC), 2015
[6] Schrödl M., Weinmeier P.: Sensorless control of reluctance machine at arbitrary operation conditions including standstill, IEEE Transactions on Power Electronics, vol. 9, no. 2, 1994
[7] Hofer M., Spiessberger R., Schroedl M.: Design and Sensorless Control of a Reluctance Synchronous Machine for a Magnetically Levitated Drive, Proceedings of the 2015 IEEE International Electric Machines and Drives Conference (IEMDC), May 2015
[8] Hofer M., Nikowitz M., Schrödl M.: Application of a Position Sensorless Control to a Reluctance Synchronous Drive Including Flux Weakening, Proceedings of 2017 International Exhibition and Conference for Power Electronics, Intelligent Motion, Renewable Energy and Energy Management, PCIM, 2017
[9] Villet W.T., Kamper M.J.: Design of a Reluctance Synchronous Machine for Saliency Based Position Sensorless Control at Zero Reference Current, IEEE International Conference on Industrial Technology (ICIT), 2013
[10] Guan Y., Zhu Z.Q., Afinowi I.A.A., Mipo J.C., Farah P.: Design of Synchronous Reluctance and Permanent Magnet Synchronous Reluctance Machines for Electric Vehicle Application, The 17th International Conference on Electrical Machines and Systems (ICEMS), 2014
[11] Howard E., Kamper M.J., Gerber S.: Asymmetric Flux Barrier and Skew Design Optimization of Reluctance Synchronous Machines, IEEE Transactions on Industry Applications, Vol. 51, no. 5, 2015
[12] Hofer M., Schrödl M.: Optimization of a Synchronous Reluctance Machine for an Industrial Drive Application Regarding to Sensorless Control, EPE'2017, ECCE Europe 2017
[13] Hofer M., Nikowitz M., Schrödl M.: Auslegung einer Einzelpol-Synchron-Reluktanzmaschine hinsichtlich sensorlosen Betriebs eines industriellen Antriebs, Elektrotechnik und Informationstechnik (E u. I), vol. 135, issue 2, Springer Verlag Wien, 2018